



Virginia Commonwealth University
VCU Scholars Compass

Electrical and Computer Engineering Publications

Dept. of Electrical and Computer Engineering

2007

Defect reduction in GaN epilayers grown by metal-organic chemical vapor deposition with in situ SiN_x nanonetwork

Jinqiao Xie

Virginia Commonwealth University

Serguei A. Chevtchenko

Virginia Commonwealth University

Ü. Özgür

Virginia Commonwealth University, uozgur@vcu.edu

Hadis Morkoç

Virginia Commonwealth University, hmorkoc@vcu.edu

Follow this and additional works at: http://scholarscompass.vcu.edu/egre_pubs

 Part of the [Electrical and Computer Engineering Commons](#)

Xie, J., Chevtchenko, S.A., Ozgur, U., et al. Defect reduction in GaN epilayers grown by metal-organic chemical vapor deposition with in situ SiN_x nanonetwork. *Applied Physics Letters*, 90, 292112 (2007). Copyright © 2007 AIP Publishing LLC.

Downloaded from

http://scholarscompass.vcu.edu/egre_pubs/102

This Article is brought to you for free and open access by the Dept. of Electrical and Computer Engineering at VCU Scholars Compass. It has been accepted for inclusion in Electrical and Computer Engineering Publications by an authorized administrator of VCU Scholars Compass. For more information, please contact libcompass@vcu.edu.

Defect reduction in GaN epilayers grown by metal-organic chemical vapor deposition with *in situ* SiN_x nanonetwork

Jinqiao Xie, Serguei A. Chevtchenko, Ümit Özgür, and Hadis Morkoç^{a)}

Department of Electrical and Computer Engineering, Virginia Commonwealth University, Richmond, Virginia 23284, and Department of Physics, Virginia Commonwealth University, Richmond, Virginia 23284

(Received 25 April 2007; accepted 5 June 2007; published online 28 June 2007)

Line and point defect reductions in thin GaN epilayers with single and double *in situ* SiN_x nanonetworks on sapphire substrates grown by metal-organic chemical vapor deposition were studied by deep-level transient spectroscopy (DLTS), augmented by x-ray diffraction (XRD), and low temperature photoluminescence (PL). All samples measured by DLTS in the temperature range from 80 to 400 K exhibited trap A (peak at ~ 325 K) with an activation energy of 0.55–0.58 eV, and trap B (peak at ~ 155 K) with an activation energy of 0.21–0.28 eV. The concentrations of both traps were much lower for layers with SiN_x nanonetwork compared to the reference sample. The lowest concentration was achieved for the sample with 6 min deposition SiN_x nanonetwork, which was also lower than that for a sample prepared by conventional epitaxial lateral overgrowth. In concert with the DLTS results, PL and XRD linewidths were reduced for the samples with SiN_x network indicating improved material quality. Consistent trend among optical, structural, and DLTS results suggests that SiN_x network can effectively reduce both point and line defects.

© 2007 American Institute of Physics. [DOI: 10.1063/1.2753096]

Despite great progress, the potential of GaN-based devices has not yet been fully realized due to the absence of native substrates and resultant defects.¹ Thin GaN layers grown on SiC or sapphire substrates typically have dislocation densities in the 10^9 – 10^{10} cm⁻² range. Since a lower defect density is required for device applications, various methods have been used to improve layer quality, such as preparation of very thick layers by hydride vapor phase epitaxy (HVPE) and epitaxial lateral overgrowth (ELO) by metal-organic chemical vapor deposition (MOCVD).² Recently, new techniques employing *ex situ* porous TiN_x (Ref. 3) or *in situ* SiN_x (Refs. 4–6) networks as nanoscale lateral overgrowth masks have paved the way for reduction of threading dislocations (TDs) as determined by transmission electron microscopy (TEM).⁷ While TEM investigations received extensive attention, systematic investigations of point defects acting as deep electron traps and nonradiation recombination centers have been lagging behind structural investigations. In this letter, the effect of SiN_x nanonetworks on the defect reduction was studied by using deep-level transient spectroscopy (DLTS) assisted by atomic force microscopy (AFM), photoluminescence (PL), and x-ray diffraction (XRD) methods.

The GaN samples were grown on sapphire substrates in a low pressure vertical MOCVD system.^{8,9} In this letter, two samples with single (5 and 6 min) and one with double (5 + 5 min) SiN_x nanonetwork interlayers (see Fig. 1) were investigated and compared to a standard ELO sample and a control sample without ELO. As reported,⁹ the minimum thickness for overgrown GaN to achieve a fully coalesced surface depends on the SiN_x coverage which is simply controlled by its deposition time. For a 5 min SiN_x (nominal thickness: ~ 2 nm) deposition time, ~ 3 μ m overgrowth is required to achieve a fully coalesced surface across the wafer for the particular growth conditions used. 6 min SiN_x depo-

sition time required an ~ 6 μ m overgrowth because of sparse nucleation sites.⁹ In the case of the sample with double SiN_x nanonetwork layers, the second SiN_x layer was deposited after coalescence of the first overgrown GaN layer (~ 3 μ m), and the total thickness of the sample was ~ 8 μ m. An ~ 6 - μ m-thick GaN sample grown directly on a low-temperature buffer layer was used as the reference sample, and an ~ 8 - μ m-thick sample prepared by conventional ELO (4/10 μ m window/wing width) was also used for benchmarking. All samples were characterized by XRD, AFM, and PL in addition to DLTS. Steady state PL was excited with the 325 nm line of a He–Cd laser and measured at 15 K in a closed-cycle optical cryostat. Undoped GaN wafers were reloaded into the MOCVD chamber for deposition of 500 nm GaN:Si [$n \sim (0.5-1) \times 10^{17}$ cm⁻³] for DLTS measurements. Then, planar Schottky diodes (200 μ m diameter) were fabricated using standard photolithography. Ti/Al/Ti/Au (30/100/30/30 nm) Ohmic contacts were deposited and annealed at 900 °C for 60 s in nitrogen ambient, followed by the deposition of Ni/Au (30/100 nm) Schottky contacts.

Figure 2 shows the typical AFM image for the 6 min SiN_x nanonetwork sample prior to the top GaN:Si layer growth. Compared to samples with 5 min or double (5+5 min) SiN_x nanonetwork, the sample with 6 min SiN_x

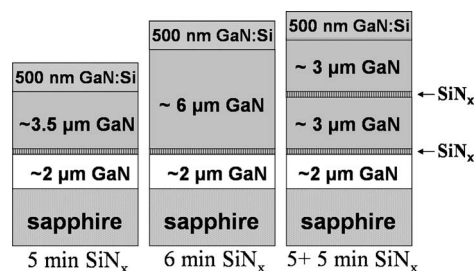


FIG. 1. Investigated GaN sample structures with single or double SiN_x nanonetworks. The topmost 500 nm GaN:Si layers with $n \sim (0.5-1) \times 10^{17}$ cm⁻³ were deposited for the DLTS measurements.

^{a)}Electronic mail: hmorkoc@vcu.edu

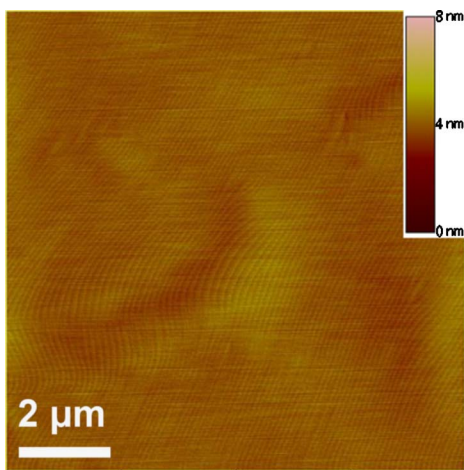


FIG. 2. (Color online) AFM image of an undoped GaN film with 6 min SiN_x nanonetwork. Predominantly straight and parallel atomic steps are clearly observed (rms: ~ 0.28 nm over a $100 \mu\text{m}^2$ area).

exhibited parallel and straight atomic steps over a relatively large area, as shown in Fig. 2, which typically is indicative of a lower dislocation density. Similarly, when the SiN_x deposition time was increased from 5 to 6 min, the XRD rocking curve full width at half maximum (FWHM) values of (002), (102), and (302) diffractions decreased from 217, 211, and 245 to 205, 192, and 221 arc sec, respectively. The XRD FWHM values for the sample with double SiN_x are similar to the one with single 5 min SiN_x . Moreover, unlike the conventional ELO samples, no c -axis wing tilt is present in the samples with SiN_x nanonetwork which conveniently facilitates correlation of rocking curve FWHM values with dislocation densities directly. From an etch pit density (EPD) study,¹⁰ the total dislocation density was estimated as $\sim (3-4) \times 10^7 \text{ cm}^{-2}$ for the sample with 6 min SiN_x and $\sim (5-6) \times 10^7 \text{ cm}^{-2}$ for the sample with 5 min single or double SiN_x , which agrees well with that obtained from the plan-view TEM study.⁹

To investigate the effect of SiN_x nanonetworks on the reduction of electron traps, DLTS measurements were performed. The current-voltage (I - V) characteristics of Schottky diodes used for the aforementioned measurements were first studied at room temperature. The majority of the diodes fabricated using GaN with SiN_x nanonetworks had leakage currents in the 10^{-9} A range at -5 V. The leakage current was in the 10^{-6} A range for the sample grown on a standard template without SiN_x . The Schottky barrier height calculated from I - V and C - V measurements was ~ 1.0 eV for the samples with SiN_x interlayers, while it was only ~ 0.8 eV for the reference sample. Furthermore, smaller ideality factors (1.03–1.08) were achieved for SiN_x nanonetwork samples compared to the reference sample (~ 1.2 – 1.3), indicative of improved Schottky diode quality on GaN with SiN_x nanonetworks.¹¹ Schottky diodes with low leakage currents were used for DLTS measurements. For each sample, the bias voltage was chosen to probe the top 200–300 nm from the surface, and the DLTS pulse's amplitude and width were adjusted to fill electron traps. Figure 3 compares the DLTS spectra for the reference sample and samples with single and double SiN_x nanonetwork layers as well as the ELO template. The dominant trap A for all the layers under study has a peak at ~ 325 K in the DLTS spectra. The activation energy for this trap determined from Arrhenius plots varied

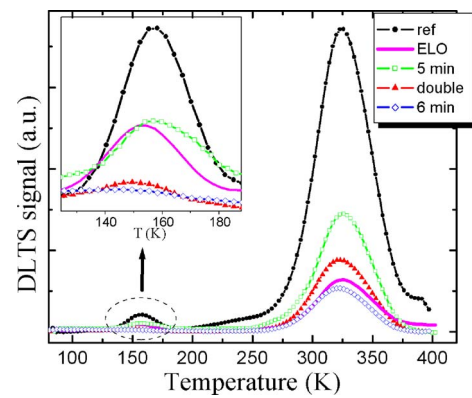


FIG. 3. (Color online) Comparison of the DLTS spectra obtained for the GaN:Si grown on different templates: the reference sample, the samples with single 5 and 6 min SiN_x , the sample with double SiN_x (5+5 min), and the ELO sample. The rate window for all spectra is 120 s^{-1} .

from 0.55 to 0.58 eV for different layers with the capture cross sections being in the low 10^{15} cm^2 range. This trap is similar to E_2 (0.58 eV),¹² D_2 (0.60 eV),¹³ and B (0.62 eV) (Ref. 14) traps commonly observed in HVPE-, MOCVD-, and molecular-beam-epitaxy-grown n -GaN layers. Hacke *et al.*¹² suggested that this trap might be related to the substitutional nitrogen atom on the Ga site. This correlation stems from the close agreement between the experimental and theoretical (0.54 eV) (Ref. 15) values for the activation energy. It was also suggested that this trap might be related to the Ga source used for growth, as it disappeared when triethylgallium (TEGa) was used instead of TMGa.¹⁶ However, these are all indirect deductions and the origin of this trap still remains unclear. Peak B (inset of Fig. 3) located at ~ 155 K corresponds to a trap with an activation energy of 0.21–0.28 eV, which has also been observed previously in GaN grown by different techniques.^{12,17} The concentration of this trap was nearly two orders of magnitude lower than that of the dominant trap A for all the samples investigated.

The concentrations of both traps A and B were the highest for the reference sample and the lowest for the sample with 6 min SiN_x nanonetwork. Together with the XRD and TEM results,⁹ the reduction of electron trap concentration for samples with SiN_x network compared to the reference sample is indicative of the link between extended defects and DLTS active traps. Since SiN_x nanonetwork reduced the nucleation sites and enlarged the grain size, the dislocation density related to the grain boundaries, and consequently electron traps and other recombination centers affected by dislocations, would be effectively reduced.⁹ Typically, there are two mechanisms TDs can affect the electron traps. First, TDs themselves can act as electron traps. It has been theoretically shown that the edge TDs in n -GaN can exist with a variety of core structures (full core, open core, Ga vacancy, and N vacancy) and induce several states in the band gap acting as electron traps.^{18,19} The activation energies determined from Arrhenius plots for the deep levels in our samples suggest that trap A could be caused by full-core and N-vacancy edge dislocations and trap B by Ga- and N-vacancy edge dislocations.¹⁹ In addition, experimental results suggested that screw and mixed-type dislocations were also responsible for trap B.²⁰ Second, due to the strong stress field in the vicinity of dislocations, point defects could be captured by TDs to form deep levels.²¹ Our preliminary studies,²² which demonstrated selective filling of trap A with

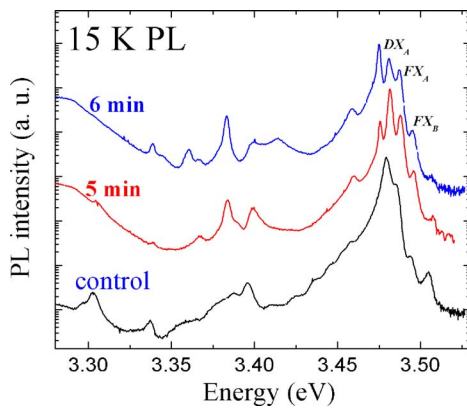


FIG. 4. (Color online) Typical near band edge PL spectra at 15 K for samples with 5 and 6 min SiN_x single interlayers and a control sample without SiN_x . The spectra were displaced vertically for clarity.

the logarithmic capture mechanism for up to ~ 20 ms filling pulse widths, supported this premise. The long filling pulse at which the saturation occurs indicates the presence of a repulsive potential most probably due to close proximity of defects responsible for trap A along the dislocations.²⁰ Regardless of the actual mechanism, the concentration of the electron traps affected by TDs would be reduced if the dislocations were significantly reduced. Therefore, supported by the fact that the sample with 6 min SiN_x has fewer TDs [$\sim (3-4) \times 10^7 \text{ cm}^{-2}$, estimated from the EPD] than the sample with 5 min SiN_x (EPD and TEM $\sim 6 \times 10^7 \text{ cm}^{-2}$) and the reference sample without SiN_x (EPD $\sim 1 \times 10^9 \text{ cm}^{-2}$), the reduction of deep levels can be explained mainly by dislocation reduction. According to XRD and AFM/EPD results, the sample with double (5+5 min) SiN_x nanonetwork layers has a dislocation density similar to that with single 5 min SiN_x nanonetwork layer (since the reduction efficiency is mainly limited by SiN_x coverage), but it has less trap A density, as shown in Fig. 3. This suggests that the second SiN_x nanonetwork layer can reduce point defects without further reducing the dislocations, which is consistent with the observation of increasing carrier lifetimes with a second SiN_x nanonetwork.⁹ The sample with 6 min SiN_x nanonetwork has the smallest trap A concentration among all the samples including the ELO sample. The dependence of trap B on the sample structure is similar to that of trap A. Our results therefore suggest that, for electron trap reduction, increasing the SiN_x coverage (e.g., from 5 to 6 min deposition) in a single layer is a more effective approach than adding a second nanonetwork layer with the same SiN_x coverage (double 5 min SiN_x nanonetworks).

To investigate the effectiveness of the SiN_x nanonetwork on the optical quality we also measured the low temperature PL spectra of the undoped samples with SiN_x nanonetwork, all of which exhibited similar excitonic features around the band edge. Figure 4 shows the excitonic region of the PL spectrum measured at 15 K for the samples with 5 and 6 min SiN_x nanonetwork interlayers and a control sample without SiN_x . The spectrum for the 6 min SiN_x nanonetwork sample contains peaks at 3.485, 3.494, and 3.505 eV which correspond to A-free exciton (FX_A), B-free exciton (FX_B), and FX_A excited state transitions, respectively,^{23,24} which are sharper than those for the control layer. The linewidth of the

DX_A peaks (3.481 eV) was reduced from ~ 4 (control sample) to < 2.5 meV with the inclusion of the 5 or 6 min SiN_x nanonetwork interlayers.

In summary, line and point defect reductions in GaN epilayers by employing *in situ* SiN_x nanonetwork were studied by DLTS augmented by AFM, XRD, and low temperature PL. DLTS data demonstrated the reduction of deep levels by the insertion of SiN_x nanonetwork. The sample with 6 min SiN_x nanonetwork layer exhibited the lowest trap concentrations (traps A and B), even lower than those for the sample prepared by conventional ELO. Our results also suggest that a more effective way to reduce both point and extended defects is to increase the SiN_x coverage in a single layer instead of adding a second SiN_x nanonetwork with the same SiN_x coverage.

This work has been funded by a grant from the Air Force Office of Scientific Research (Kitt Reinhardt). The authors thank T. S. Kuan, W. J. Choyke, R. M. Feenstra, and R. Devaty for discussions and collaborations on the dislocation reduction in GaN growth, and D. Johnstone for continual discussions of DLTS.

¹H. Morkoç, *Nitride Semiconductors and Devices*, 2nd ed. (Springer, New York, to be published).

²P. Gibart, Rep. Prog. Phys. **67**, 667 (2004).

³Yi Fu, T. Moon, F. Yun, Ü. Özgür, J. Q. Xie, S. Dogan, H. Morkoç, C. K. Inoki, T. S. Kuan, L. Zhou, and D. J. Smith, Appl. Phys. Lett. **86**, 043108 (2005).

⁴S. Sakai, T. Wang, Y. Morishima, and Y. Naoi, J. Cryst. Growth **221**, 334 (2000).

⁵S. Haffouz, H. Lahrèche, P. Vennéguès, P. de Mierry, B. Beaumont, F. Omnès, and P. Gibart, Appl. Phys. Lett. **73**, 1278 (1998).

⁶X. L. Fang, Y. Q. Wang, H. Meidia, and S. Mahajan, Appl. Phys. Lett. **84**, 484 (2004).

⁷K. Pakuła, R. Bożek, J. M. Baranowski, J. Jasinski, and Z. Liliental-Weber, J. Cryst. Growth **267**, 1 (2004).

⁸Y.-T. Moon, J. Xie, C. Liu, Y. Fu, X. Ni, N. Biyikli, K. Zhu, F. Yun, H. Morkoç, A. Sagar, and R. M. Feenstra, J. Cryst. Growth **291**, 301 (2006).

⁹J. Xie, Ü. Özgür, Y. Fu, X. Ni, H. Morkoç, C. K. Inoki, T. S. Kuan, J. V. Foreman, and H. O. Everitt, Appl. Phys. Lett. **90**, 041107 (2007).

¹⁰P. Visconti, K. M. Jones, M. A. Reshchikov, R. Cingolani, H. Morkoç, and R. J. Molnar, Appl. Phys. Lett. **77**, 3532 (2000).

¹¹J. Xie, Y. Fu, X. Ni, S. Chevtchenko, and H. Morkoç, Appl. Phys. Lett. **89**, 152108 (2006).

¹²P. Hacke, T. Detchprohm, K. Hiramatsu, N. Sawaki, K. Tadatomo, and K. Miyake, J. Appl. Phys. **76**, 304 (1994).

¹³D. Haase, M. Schmid, W. Kürner, A. Dörnen, V. Härle, F. Scholz, M. Burkard, and H. Schweizer, Appl. Phys. Lett. **69**, 2525 (1996).

¹⁴Z.-Q. Fang, D. C. Look, W. Kim, Z. Fan, A. Botchkarev, and H. Morkoç, Appl. Phys. Lett. **72**, 2277 (1998).

¹⁵D. W. Jenkins and J. D. Dow, Phys. Rev. B **39**, 3317 (1989).

¹⁶W. I. Lee, T. C. Huang, J. D. Guo, and M. S. Feng, Appl. Phys. Lett. **67**, 1721 (1995).

¹⁷W. Götz, N. M. Johnson, H. Amano, and I. Akasaki, Appl. Phys. Lett. **65**, 463 (1994).

¹⁸A. F. Wright and U. Grossner, Appl. Phys. Lett. **73**, 2751 (1998).

¹⁹S. M. Lee, M. A. Belkhir, X. Y. Zhu, Y. H. Lee, Y. G. Hwang, and T. Frauenheim, Phys. Rev. B **61**, 16033 (2000).

²⁰C. B. Soh, S. J. Chua, H. F. Lim, D. Z. Chi, W. Liu, and S. Tripathy, J. Phys.: Condens. Matter **16**, 6305 (2004).

²¹P. Omling, E. R. Weber, L. Montelius, H. Alexander, and J. Michel, Phys. Rev. B **32**, 6571 (1985); J. F. Barbot, P. Girault, C. Blanchard, and I. A. Hümmelgen, J. Mater. Sci. **30**, 3471 (1995).

²²S. A. Chevtchenko, J. Xie, Y. Fu, X. Ni, H. Morkoç, and C. W. Litton, Proc. SPIE **6473**, 64730N (2007).

²³Ü. Özgür, Y. Fu, Y. T. Moon, F. Yun, H. Morkoç, and H. O. Everitt, J. Appl. Phys. **97**, 103704 (2005).

²⁴M. A. Reshchikov and H. Morkoç, J. Appl. Phys. **97**, 061301 (2005).